REGULAR ARTICLE

Identification and characterization of *DSPIa*, a novel isoform of human *desmoplakin*

Rita M. Cabral · Hong Wan · Clare L. Cole ·
Dominic J. Abrams · David P. Kelsell · Andrew P. South

Abstract Desmoplakin is a ubiquitous component of desmosomes and desmosome-like structures, such as the cardiomyocyte area composita. Two major isoforms, desmoplakin I (DSPI) and desmoplakin II (DSPII) are encoded by alternative mRNA transcripts differentially spliced from the same gene. The resulting proteins are identical in amino acid sequence with the exception that DSPII contains only one third of the central alpha-helical rod domain present in DSPI. Here we describe a novel minor isoform of desmoplakin that is also produced by alternative splicing of the *desmoplakin* gene and that we name *desmoplakin Ia* (*DSPIa*). *DSPIa* is an alternatively spliced *DSPI* mRNA with a unique splice donor site that is 90% homologous to and downstream of the *DSPII* specific donor. The resulting *DSPIa* mRNA is in-frame and encodes a protein that has a central alpha-helical rod domain of intermediate size and that is 156 amino acids larger than DSPII and 443 amino acids smaller than DSPI. We demonstrate, through recombinant expression and short interfering RNA knockdown, that the DSPIa protein is readily detectable, albeit at substantially lower levels than the dominant isoforms, DSPI and DSPII. *DSPIa* mRNA has a similar tissue distribution to that of *DSPI* and of *DSPII*.

Keywords Desmosome · Desmoplakin · Isoform · Splice site · Quantitative polymerase chain reaction · Human

R. M. Cabral · D. P. Kelsell · A. P. South
Centre for Cutaneous Research,
Blizard Institute of Cell and Molecular Science,
University of London,
London, UK

H. Wan
Centre for Clinical and Diagnostic Oral Sciences,
Institute of Dentistry, Bart's and The London
School of Medicine and Dentistry, University of London,
London, UK

C. L. Cole · A. P. South (✉)
Centre for Oncology & Molecular Medicine,
University of Dundee, Ninewells Hospital & Medical School,
Dundee DD1 9SY, UK
e-mail: a.p.south@dundee.ac.uk

D. J. Abrams
Department of Cardiac Electrophysiology,
St Bartholomew's Hospital,
London, UK

Introduction

Desmoplakin (DSP) is a key junctional protein necessary for the morphogenesis and integrity of epithelial and vascular tissues, being a linker protein providing attachment for cytoskeletal elements such as intermediate filaments (IFs; Getsios et al. 2004). DSP ablation in mice results in an embryonic lethal phenotype (Gallicano et al. 1998), whereas conditional targeting to the epidermis leads to severe trauma-induced intercellular separation (Vasioukhin et al. 2001). Human mutations in the DSP gene can result in a range of clinical phenotypes (Cabral and South 2009); from striate palmoplantar keratoderma (Armstrong et al. 1999; Whittock et al. 1999), a mild skin condition, to sudden death from heart defects (Norgett et al. 2000, 2006; Uzumcu et al.

2006), through to early lethality as a result of devastating skin blistering and subsequent water loss (Jonkman et al. 2005). DSP is a ubiquitous component of desmosomes and desmosome-like structures, such as the cardiomyocyte area composita (Angst et al. 1990; Franke et al. 1982, 2006). Two major isoforms, desmoplakin I (DSPI) and desmoplakin II (DSPII) are encoded by alternative mRNA transcripts differentially spliced from the same gene (Green et al. 1990). Although usually expressed together, DSPI is the predominant isoform in heart (Angst et al. 1990; Uzumcu et al. 2006). DSPI and DSPII differ only in the size of the central alpha-helical rod domain, DSPII having two thirds fewer amino acids within this domain (Green et al. 1990). Human mutation leading to DSPI ablation while leaving DSPII intact results in severe arrhythmogenic right ventricular cardiomyopathy (ARVC) and early heart failure coupled with a mild skin phenotype of woolly hair and palmoplantar keratoderma in a single patient aged 4 years. These data reveal the importance of DSPI in heart tissue but highlight the ability of DSPII to support early heart development and to maintain skin homeostasis in inter-follicular epidermis (Uzumcu et al. 2006).

Here, we described the identification and characterisation of a novel human DSP isoform, DSPIa. DSPIa is expressed as a result of an in-frame alternative splice donor site within the DSPI gene. DSPIa mRNA encodes a protein identical to DSPI and DSPII with the exception of the central alpha-helical rod domain, which is of intermediate size, being 156 amino acids larger than DSPII and 443 amino acids smaller than DSPI. This new isoform has been previously overlooked presumably because of similarities in molecular weight and a much reduced expression level compared with DSPI and DSPII. We describe the tissue distribution of DSPIa, showing it to be similar to that of DSPI and of DSPII, and demonstrate that DSPIa is detected in protein lysates from epidermal cells and heart tissue.

Materials and methods

Reverse transcription with polymerase chain reaction

RNA was isolated from frozen skin sections by using the RNAeasy mini kit (Qiagen, Calif., USA) and from cultured cells at 70%–90% confluency by using the RNA-Bee reagent (AMS Biotechnology, Spain) according to the manufacturers' specifications. cDNA was generated by using M-MLV reverse transcription (RT; Promega, Calif., USA). RT-polymerase chain reaction (RT-PCR) for expression profiling of DSP isoforms in a range of tissues was carried out on normal skin cDNA isolated as described and on Human Multiple Tissue cDNA panel 1

and Human Cardiovascular Multiple Tissues cDNA panel (BD Biosciences, N.J., USA). The G3PDH (glyceraldehyde-3-phosphate dehydrogenase) gene was amplified as a control of cDNA abundance according to the manufacturer's specifications. Primers, which amplified cDNA corresponding to DSPI, DSPIa and DSPII isoforms, were as follows: DSPIF, 5′ CTTGGAACTAAGGAGCCAG; DSPIaF, 5′ GCTTGA TAGACTTTCAAGGG; DSPIIF, GATCGAAGTTTTG GAAGAGG; DSPR, CCACCTGAGTACACTGATTC.

Quantitative PCR

Human liver and aorta total RNA was purchased from Clontech (BD Biosciences) and human ventricle and atrium total RNA was purchased from AMS Biotechnology Europe (Abingdon, UK). cDNA was constructed as described. Real-time quantitative PCR was performed by using the MiniOpticon detection system (Bio-Rad, UK) and the DyNAmo SYBR Green qPCR kit (Finnzymes, Finland). DSP isoform-specific primers were as described above. EF1alpha or B2M were used as reference genes. Cycling conditions were according to the manufacturer's instructions. Relative quantification was established by defining the difference between the reference and target cycle threshold values for each sample.

Immunoblotting

Small fragments of redundant atrium tissue were obtained during cardiac surgery and transported to the laboratory in dry ice. These small fragments were solubilised into an appropriate volume of 0.1 M TRIS-HCl pH 6.8, 0.2 M dithiothreitol, 4% (w/v) SDS, 0.2% (w/v) bromophenol blue and 20% (v/v) glycerol and subsequently boiled for 5 min before resolution on NuPAGE Novex 3%–8% TRIS-acetate Mini gels according to the manufacturer's specifications (Invitrogen, The Netherlands). Whole-cell protein extracts were prepared from cells lysed in 0.125 M TRIS-HCl pH 6.8, 4% (w/v) SDS, 20% (v/v) glycerol, 0.001% (w/v) bromophenol and 1.44 M β-mercaptoethanol, boiled for 5 min and resolved on SDS-PAGE as described. The primary antibody used was 11-5F (mouse monoclonal anti-DSPI and DSPII), a generous gift from David Garrod (Parrish et al. 1987).

Recombinant DSPIa expression

DSPIa was cloned from primary human keratinocyte RNA by using standard molecular biology techniques. The use of the pBabe-puro retroviral vector (Morgenstern and Land 1990) and phoenix packaging system (Kinsella and Nolan 1996) to introduce full length DSPIa was as described elsewhere (South et al. 2003).

Transfections with short interfering RNA

Isoform-specific short interfering RNAs (siRNAs) were designed by using the custom siRNA design tool from Thermo Fisher Scientific (Waltham, Mass., USA) according to the manufacturer's specifications. siRNA sequences targeting *DSPI/DSPIa* were as follows: si2, ATAAGGA GATCGAGAGACT; si3, GGCCTGTGGCTCTGAGATA; si4, AGATAGAACTGAAGCAGGT. siRNA sequences targeting *DSPI* were as follows: si*DSPI* 1, GAGCTTATCT GAAGAAATA; si*DSPI* 2, CGAACAGAGGAGAGCG TAA. The siRNA designated as siI/II, which targets all three isoforms, was published previously (Wan et al. 2007). Transient transfections of HaCaT cells were performed according to the DharmaFECT general transfection protocol (Thermo Fisher Scientific, UK) for a 6-well plate format. Briefly, 2×10^5 cells per well of a 6-well dish were seeded and incubated in antibiotic-free medium containing fetal bovine serum, at 37°C, for 24 h prior to siRNA transfection. In separate polystyrene tubes, 100 nM siRNA (final concentration) and 6 μl DharmaFECT 1 were mixed in serum- and antibiotic-free media and incubated at room temperature for 5 min. The siRNA-containing medium was added to the tube containing the DharmaFECT 1 reagent and these contents were mixed and incubated for 20 min at room temperature. Serum-containing media was added to the mix and the cells were incubated in this siRNA-containing media for 4 days and subsequently prepared for Western blot. Cells transfected with a pool of four non-targeting siRNAs (on target plus siControl non-targeting pool) and cells incubated with DharmaFECT 1 transfection reagent only (mock) were used as negative controls.

Results

RT-PCR amplification of a shorter *DSPI* cDNA

While cloning *DSPI*, we amplified a shorter than expected cDNA product by using *DSPI*-specific PCR primers. Direct sequencing revealed this PCR product was 1329 bp shorter than *DSPI* but corresponded to the *DSPI* sequence. Alignment analysis showed that this shorter cDNA had been generated by splicing involving the exon 24 splice acceptor (common to *DSPI* and *DSPII*) and a previously unidentified splice donor within exon 23 of *DSPI*. The spliced *DSPI* sequence was in-frame and potentially coded for a desmoplakin protein intermediate in size between DSPI and DSPII. We named this cDNA sequence *DSPIa*. Figure 1a shows the organisation of the *DSP* gene at exons 23-24 for *DSPI*, *DSPII* and the novel *DSPIa* mRNA.

DSPIa utilises a donor splice site 90% homologous to *DSPII* and is detected in ESTs from prostate cancer cell line DU-145

Sequence analysis demonstrated that the *DSPIa* donor splice site is 90% homologous to the exon 23 donor site of *DSPII* (Whittock et al. 1999; Fig. 1a). Splice analysis of the 3000-bp region spanning the end of exon 23 and the beginning of exon 24 (see Fig. 1a) predicted *DSPII* and *DSPIa* to harbour the two most efficient splice donors with equal or highly similar prediction scores (Figs. 1b, S1a). Interestingly, neither of the splice prediction software packages that we used identified the *DSPI* donor site by using default settings (Figs. 1b, S1a). Reducing the cut-off of detection did eventually identify the *DSPI* donor site but the sequence gave a considerably lower value than *DSPII*, *DSPIa* and other potential splice donor sites within this region (Fig. S1b, data not shown).

In order to establish whether *DSPIa* was present in the EST database (dbEST; Boguski et al. 1993), we searched for *DSP* sequences by using the BLAST 2.2.22 megablast program (accessed from http://blast.ncbi.nlm.nih.gov/Blast.cgi on 17-02-2010; Zhang et al. 2000). Using 50 bp spanning each of the three isoform unique exon-exon junctions, we identified 36 separate human EST entries for *DSPI*, five separate human entries for *DSPII* and one human entry for *DSPIa*. The prostate cancer cell line EST homologous to *DSPIa* (accession AI525952) was of poor sequence quality but displayed 86% homology over 342 bp spanning the *DSPIa* exon-exon boundary by using the BLAST 2.2.22 blastn program (accessed on 17-02-2010; Altschul et al. 1997). Continuous homology between this EST and *DSPI* or *DSPII* did not extend across exon-exon boundaries demonstrating that this EST represented *DSPIa* and that *DSPIa* is expressed in the prostate cancer cell line DU-145. Figure 1c depicts the number of human EST identified by searching dbEST with the corresponding sequences.

DSPIa tissue distribution is similar to that of *DSPI* and of *DSPII*

To identify the extent of *DSPIa* expression in various human tissues, we designed a *DSP* isoform-specific RT-PCR (Fig. 2a). Using this RT-PCR assay, we examined the expression of *DSPIa* by using multiple tissue cDNA panels and demonstrated that *DSPIa* expression was similar to that of *DSPI* and of *DSPII* but, surprisingly, was the only isoform detected in the aorta (Fig. 2b, c).

In order to verify our findings in the aorta and to examine the relative level of *DSPIa* in cultured keratinocytes, epithelial and heart tissues, we used quantitative PCR (Q-PCR) and total RNA-derived cDNA to show that *DSPIa*
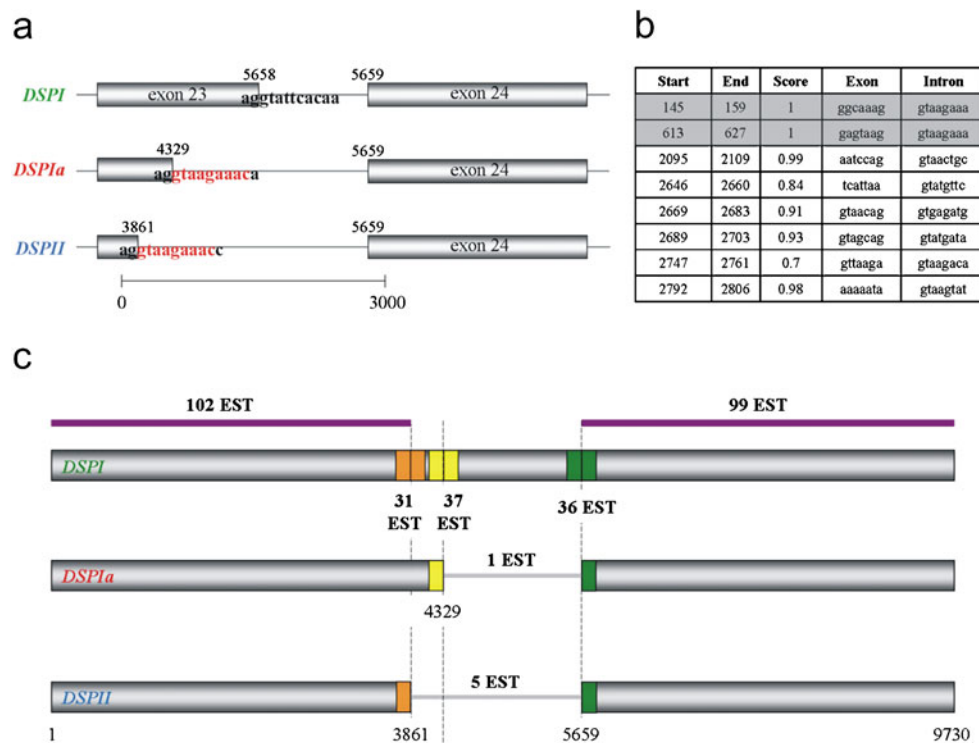
Fig. 1 Alternative splice prediction and expressed sequence tag (EST) analysis of *DSP* isoform-specific mRNA. **a** Organisation of the *DSP* gene at exons 23–24 for *DSPI*, *DSPII* and the novel *DSPIa* splice variant. The sequences of three splice donors in exon 23 that produce the different splice isoforms are shown (*red* shared nucleotides). **b** Splice donor analysis of 3000 bp of sequence spanning intron 23 of the *DSP* gene, indicated in **a**, (NNSPLICE version 0.9 accessed via http://www.fruitfly.org/seq_tools/splice.html; Reese et al. 1997) identifies the splice donor sites used by *DSPII* and *DSPIa* (*grey*) but not *DSPI*. **c** Representation of *DSP* splice variants showing ESTs found in the NCBI database; 5′ and 3′ regions (*purple*) are represented by 102 and 99 ESTs, respectively. The *DSPIa*- and *DSPII*-specific junctions (*yellow/green* and *orange/green*) are spanned by 1 and 5 ESTs, respectively. The corresponding *DSPI*-specific junctions are represented by 37 (*yellow*) and 31 (*orange*) ESTs, respectively. The *DSPI*-specific exon 23/24 junction (*green*) is represented by 36 ESTs. Each *coloured square* comprises 25 bp each side of the *dashed line*

relative to *DSPI* levels are similar when comparing epidermal keratinocyte cells and cell lines (ratio: 3–7 per relative 100 *DSPI*) but that the relative level of *DSPIa* in simple epithelial tissue (liver) and heart was lower (ratio: 0.1–2 per relative 100 *DSPI*; Fig. 2d). Using this approach, we were able to detect *DSPI* and *DSPIa* in the aorta and show that the expression of both these DSP isoforms was significantly lower compared with other heart compartments (Fig. 2e).

DSPIa is expressed in epidermal keratinocytes and heart tissue

Because of the size and similarity of DSP proteins, we speculated that DSPIa might have previously been over-looked in Western blotting because of co-migration and relative abundance. We therefore resolved total protein lysates from cultured human epidermal keratinocytes and human atrium tissue on 3%–8% gradient TRIS-Acetate gels for a considerably longer time than we would normally. Immunoblotting with a specific DSP antibody identified a

faint immunoreactive band of the expected size for DSPIa (Fig. 3a). In order to confirm that this protein was indeed DSPIa, we expressed DSPIa in A293 phoenix cells and the epidermal keratinocyte cell line, HaCaT. Recombinant DSPIa migrated at a distance corresponding to the faint immunoreactive band in HaCaT cells (Fig. 3b).

siRNA knockdown with sequences specific to *DSPI* and *DSPIa* efficiently target DSPIa

To confirm further the existence of detectable levels of DSPIa, we used siRNA specifically to inhibit the mRNA of *DSPI*, *DSPI* and *DSPIa* and all three isoforms. siRNAs si2, si3 and si4 targeting *DSPI* and *DSPIa* (Fig. S2) significantly reduced the level of both corresponding proteins (Fig. 3c), whereas siRNA targeting *DSPI* only (Fig. S2) did not effect the levels of *DSPIa* (Fig. 3d). All three isoforms were downregulated with siRNA siI/II, which targets the 5′ end of *DSP* (Fig. 3d). These data demonstrate that all immunoreactive bands are DSP-specific and that only the knockdown of DSPI does not effect DSPIa expression.

Fig. 2 *DSPIa* mRNA expression profile is similar to that of *DSPI* and of *DSPII*. **a** *Left* Genomic organisation of exons 23–24 of *DSPI*, *DSPII* and the novel *DSPIa* isoform showing primers used specifically to amplify and distinguish between the different isoforms. The reverse primer (*DSP*R, grey) is common to all isoforms. Three different forward primers (*DSPI*F, green; *DSPIa*F, red; *DSPII*F, blue) were designed specifically to amplify *DSPI* (179 bp), *DSPIa* (383 bp) and *DSPII* (530 bp), respectively. *Right* RT-PCR products and respective negative water controls amplified from *DSPI* (lanes 1, 2), *DSPIa* (lanes 3, 4) and *DSPII* (lanes 5, 6) RNA from primary NHK (*M* molecular weight marker). **b**, **c** Specific amplification of the various *DSP* transcripts across a range of tissues in human multiple tissue cDNA panels and in normal skin and HaCaT and K1 keratinocyte cell lines. *DSPIa* (383 bp) is expressed throughout the majority of epithelial tissues, normal skin and keratinocyte cell lines with similar expression patterns to that of *DSPI* (179 bp) and of *DSPII* (530 bp). *DSPIa* is also expressed in cardiovascular tissue but is the only *DSP* isoform detected in the aorta. Primers to amplify the *G3PDH* gene (983 bp according to NM_002046.3) were used as a control of cDNA abundance (*Water* negative control). **d**, **e** SYBR Green quantitative RT-PCR with forward primers *DSPI*F, *DSPIa*F and *DSPII*F and the reverse primer *DSPI*R was performed to amplify *DSPI*, *DSPIa* and *DSPII*. **d** NHK, HaCaT and K1 keratinocytes, liver, aorta, atrium and ventricle expression levels of all *DSP* isoforms relative to *DSPI* (normalised within each sample). *Error bars* indicate mean±SEM, minimum of *n*=3 in each case. **e** Relative levels of mRNA expression for each isoform are shown, comparing cultured primary keratinocytes with liver and heart. All values are normalised to NHK *DSPI*. All samples are human. *Error bars* indicate mean±SEM, minimum of *n*=3 in each case
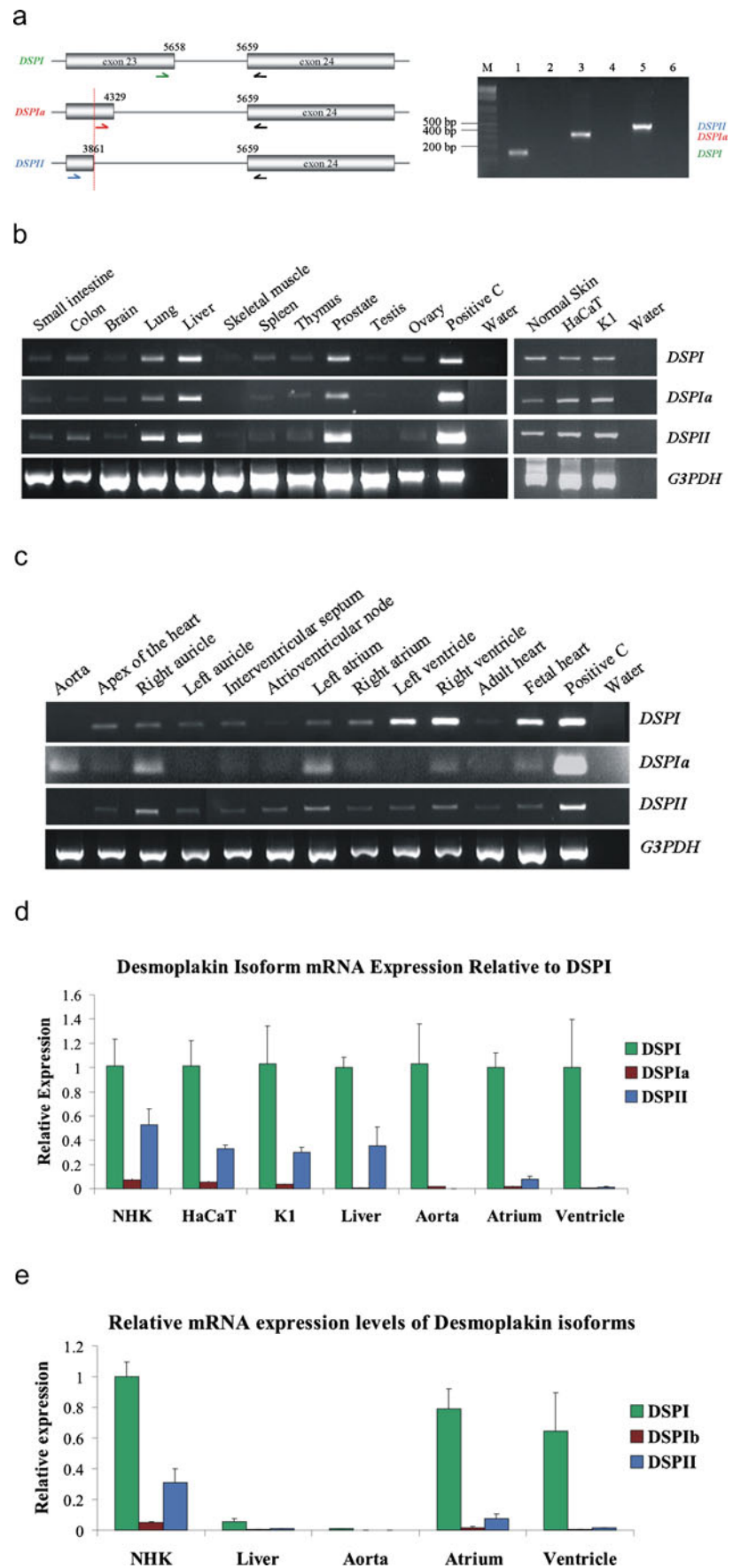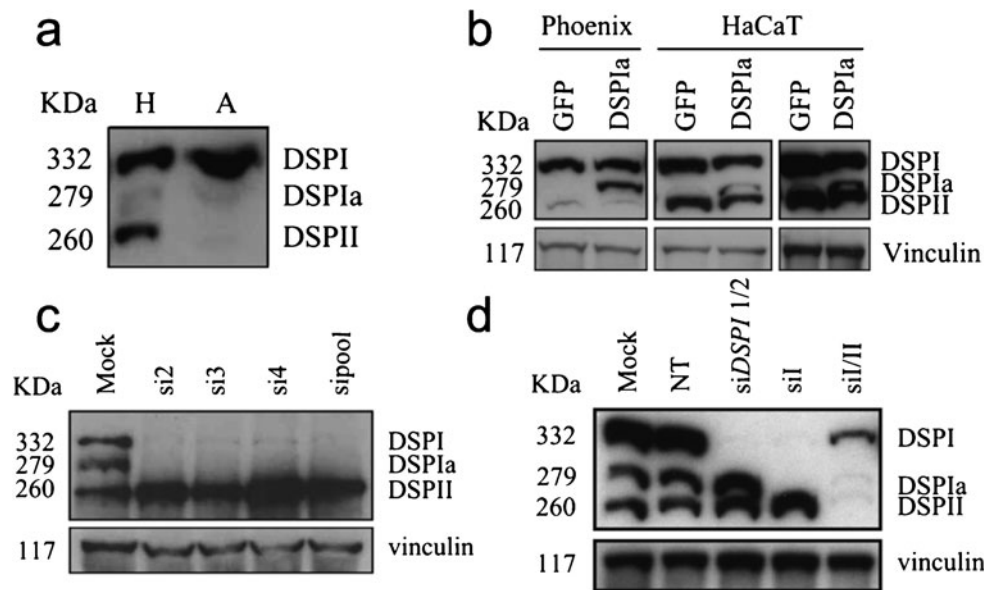
Fig. 3 DSPIa is expressed in epidermal keratinocytes and human atrium tissue. **a** Western blot of total proteins from HaCaT cells (*H*) and normal human atrium (*A*). The predicted molecular weight of each protein is indicated *left* (in kDa [*KDa*]). DSPIa is observed in HaCaT cells, together with DSPI and DSPII. Expression of DSPI and low levels of DSPIa are observed in the normal human atrium, whereas DSPII is barely detectable in this tissue. **b** Phoenix cells were transiently transfected with a pBabe-*GFP* control vector (*GFP*) and the pBabe-*DSPIa* construct (*DSPIa*). Recombinant DSPIa expression is observed in pBabe-*DSPIa* transfected cells at approximately 279 KDa. HaCaT cells transduced with the pBabe-*DSPIa* construct (*DSPIa*) show expression of recombinant DSPIa at higher levels than those of the endogenous DSPIa band in pBabe-*GFP*-transduced cells (*GFP*). Higher exposure of the same blot (*right*) shows recombinant DSPIa proteins migrate alongside endogenous DSPIa protein. Vinculin (117 KDa) was used as a loading control. **c** Western blot of total lysates from HaCaT cells transfected with 100 nM of each siRNA (*si2*, *si3*, *si4*) designed to target *DSPI/DSPIa*. Endogenous DSPI and DSPIa are downregulated with siRNAs *si2-4* (*Mock* cells incubated with DharmaFECT 1 transfection reagent only). **d** Western blot of whole cell lysates from HaCaT cells transduced with pBabe-*DSPIa* construct. DSPIa is downregulated with siRNAs that target the predicted *DSPIa* (*siI*, *siI/II*) sequence but not with siRNAs that are *DSPI*-specific (*siDSPI 1/2*)

Discussion

Pre-mRNA splicing is a mechanism of post-transcriptional regulation of gene expression by which non-coding introns are excised and exons are joined to form a mature mRNA transcript. Alternative pre-mRNA splicing is thought to occur in approximately 75% of all human genes (Johnson et al. 2003) and, by this mechanism, human cells are able to synthesise over 90,000 proteins from approximately 26,000 coding genes (Ast 2004). Many of these alternative splice variants are differentially expressed according to tissue type and developmental stage. Alternative splicing involves sequential phosphodiester transfer reactions that are catalysed by a large ribonucleoprotein complex. Three consensus sequences within each intron are required for splicing to occur; 5′ and 3′ splice sites (donor and acceptor sites, respectively) that flank each intron, and a branch point that is located more than 18 nucleotides upstream of the acceptor site and more than 48 nucleotides downstream of the donor site (Matlin et al. 2005). Here, we identify a previously undescribed DSP isoform, *DSPIa*, which is produced by alternative splicing of the *DSP* gene. Given that *DSPIa* shares its acceptor site with all isoforms of *DSP* and that its donor splice site shares 90% homology with *DSPII*, differing only in the 10th 3′ base, we speculate that the branch points differ between *DSPII* and *DSPIa*. The possibility nevertheless exists that the branch point is shared and that *DSPII* is the major splice variant because of efficiencies of the spliceosome at the most 5′ sequence but our finding of DSPIa in heart tissue in the absence of detectable DSPII (Fig. 3a) suggests a unique branch point. Following on from this logic, it is also likely that separate branch points direct the variable tissue expression of DSPI and DSPII.

Our Q-PCR data show that we are able to detect all *DSP* isoforms in all tissues tested with the exception of the aorta in which DSPII is below the threshold of detection, data in agreement with our original RT-PCR panel screen (Fig. 2c, d). This is surprising given that, so far, no DSP protein has been detected in junctions of the vascular endothelium of human vessels, with the exception of the complexus adhaerentes identified in the lymph node sinus (Moll et al. 2009). Such junctions have also been identified in the cultured human umbilical vein endothelial cell line (Valiron et al. 1996). Our finding of extremely low levels of *DSP* in aorta RNA suggests that the sensitive Q-PCR methodology is able to detect low levels of mRNA transcripts either regulated in a post-transcriptional manner or contaminating RNA from a separate compartment.

The ability to detect *DSPI* by Q-PCR but not by RT-PCR probably reflects template complexity; the RT-PCR cDNA panels used in Fig. 2b, c are produced from polyadenylated mRNA and are at low concentrations (total input approximately 5 ng), whereas the Q-PCR assay cDNA are constructed from total RNA at a concentration of around 400 ng. The lack of detectable *DSPII* is curious but, notably, PCR is dependent on the efficiency of primer binding coupled with template complexity and we cannot compare absolute levels between the different DSP isoform Q-PCR assays relative to control (Bustin 2000). A definitive demonstration of expression relies on protein detection, which in itself is dependent on antibody specificity. Here, we demonstrate the detection of DSPIa by using an antibody raised against a common DSP epitope (Parrish et al. 1987) and, although a different protein conformation may influence recognition, we feel that this is unlikely. By this method, we have detected DSPIa protein in cultured keratinocytes and heart tissue and no DSPII in heart tissue (Fig. 3a).

DSPIa has not previously been described, presumably because of multiple factors chiefly resulting from the low level of expression relative to *DSPI* and *DSPII* (which would lead to a reduced number of EST spanning intron 23 of the *DSPIa* gene, for example) but also from the difficulty in resolving DSPII protein from DSPIa by using standard Western blotting techniques. Indeed, our ability to resolve DSPIa is clearly dependent upon a number of as yet undetermined parameters; occasionally, DSPIa is particularly prominent (for example, Fig. 3c) and, at other times, it is less pronounced (Fig. 3a). However, *DSPIa* is clearly a minor isoform of *DSP* that is expressed in a wide range of human tissues, with *DSPIa* being translated into a protein that is identical to DSPI and DSPII in both the N and C terminal portions but contains only half of the DSPI alpha helical rod domain. Lack of evidence for DSPIa protein in the extensive documentation of DSP can be attributed to the widespread use of non-human tissue (Mueller and Franke 1983) and cell lines (Green et al. 1991) and insufficient protein resolution. We are, however, tempted to speculate that DSPIa has been previously identified by using Western blotting of protein lysates from FaDu cells (human upper respiratory tract tumour line) by Angst and colleagues (1990) but, again, the resolution and quantity of protein was not sufficient for conclusive evidence.

The function of the various domains of DSP has been extensively investigated (Bornslaeger et al. 1996; Fontao et al. 2003; Green et al. 1990, 1992; Kouklis et al. 1994; Kowalczyk et al. 1994; Meng et al. 1997; Smith and Fuchs 1998; Stappenbeck et al. 1993, 1994; Stappenbeck and Green 1992; Vasioukhin et al. 2001). The C-terminal domain of DSP is responsible for mediating interactions with various types of IFs: vimentin in meninges and dendritic cells of lymph nodes, desmin in the myocardium and a variety of keratins in epithelial tissues (Fontao et al. 2003; Kouklis et al. 1994; Meng et al. 1997; Stappenbeck et al. 1993; Stappenbeck and Green 1992). The N-terminal plakin domain of DSP is important for targeting DSP to the junctional plaque through interactions with the armadillo proteins plakoglobin and plakophilin (Bornslaeger et al. 2001; Kowalczyk et al. 1997, 1999) and DSP has also been shown to be able to bind itself through this domain (Smith and Fuchs 1998). However, whereas interactions with binding partners are known to be facilitated by the N- and C-terminal domains of DSP, the rod domain is thought only to be important for self-association (Green et al. 1990; O'Keefe et al. 1989). DSP isolated from pig tongue has provided evidence that DSPI can homo-dimerise in solution, whereas DSPII remains monomeric (O'Keefe et al. 1989). However, the rod domains of both DSPI and DSPII are predicted to form homophilic coiled-coil dimers (Green et al. 1990; Virata et al. 1992). Such higher order aggregates of DSP are thought to form a filamentous network that interacts with other desmosomal plaque proteins between the membrane and IFs (Getsios et al. 2004). North et al. (1999) have proposed, based on the immunogold labelling of the N- and C-termini revealing consistent spatial localisation in tissues expressing both DSPI and DSPII, that DSPII governs the thickness of the inner dense plaque and that DSPI is folded within the plaque. This logic would translate to DSPIa but the functional consequences of shortening the rod domain remain unknown. Interestingly, the detection of DSPIa in heart tissue raises the possibility that DSP protein with a shorter rod domain, regardless of overall amounts, might be necessary for desmosomal integrity. Notably, however, the assembly of desmosomal components in vitro is possible with DSPI and, therefore, DSPII and DSPIa might simply be "structural accessories" (Bornslaeger et al. 2001).

Nine human mutations have so far been reported within the rod domain of *DSP*. Two of these mutations (p.R1113X and p.R1934X) affect all three isoforms; another three (p.R1255K, p.R1267X and p.N1324fsZ23) affect DSPI and DSPIa and four (p.R1775I, p.K1583R, p.L1654P and p.Q1446X) affect only DSPI while leaving DSPIa and DSPII intact (Bolling and Jonkman 2009). Three of the mutations affecting only DSPI are missense mutations causing dominant ARVC, whereas the single nonsense mutation affecting only DSPI, p.Q1446X, causes recessive cardio-cutaneous disease when inherited with another nonsense mutation, p.Q673X, which affects all isoforms (Asimaki et al. 2009). This combination of mutations is predicted to lead to complete ablation of DSP expression from one allele (p.Q673X) and ablation of DSPI only, allowing expression of DSPII and DSPIa from the other allele (p.Q1446X). This contrasts with the homozygous p.R1267X nonsense mutation, which leads to complete absence of both DSPI and DSPIa, leaving DSPII intact, and resulting in

recessive cardio-cutaneous disease (Uzumcu et al. 2006). In this case (p.R1267X/p.R1267X), the cutaneous phenotype is relatively mild (compared with p.Q673X/p.Q1446X) presumably because of normal DSPII expression (which is haplo-insufficient in p.Q673X/p.Q1446X and results in more severe cutaneous disease). Interestingly, the cardiac phenotype might be considered more severe in p.R1267X/p.R1267X with cardiac failure at age 4 years compared with cardiac failure at age 9 years in the p.Q673X/p.Q1446X case and therefore we are tempted to speculate that these data show that expression of DSPIa, although not capable of rescuing the cardiac phenotype, can influence its severity and positively contributes towards cardiac cohesion.

The ratio between DSPI and DSPII varies among the different tissues and different cell types; DSPII, which is abundantly expressed in complex epithelial tissues, is expressed at lower levels in cells derived from some other epithelial tissues such as epidermoid carcinoma (vulva) and human bladder carcinoma (transitional epithelium; Angst et al. 1990) and in the heart (Uzumcu et al. 2006). We show here that the relative levels of *DSPI*, *DSPII* and *DSPIa* are consistent in keratinocyte-derived cells and that *DSPIa*, like DSPII relative levels, is decreased in the liver and heart compared with keratinocytes.

The majority of desmosomal genes are alternatively spliced and little is known about the role of some of these splice isoforms, such as DSC "b" proteins or indeed DSPII. A large volume of research has been published based on recombinant DSPI and whether DSPII or DSPIa has any differential biological role in cell junction formation and signalling remains to be seen. Further work will be necessary to investigate the importance and function of these isoforms.

References

Altschul SF, Madden TL, Schaffer AA, Zhang J, Zhang Z, Miller W, Lipman DJ (1997) Gapped BLAST and PSI-BLAST: a new generation of protein database search programs. Nucleic Acids Res 25:3389–3402

Angst BD, Nilles LA, Green KJ (1990) Desmoplakin II expression is not restricted to stratified epithelia. J Cell Sci 97:247–257

Armstrong DK, McKenna KE, Purkis PE, Green KJ, Eady RA, Leigh IM, Hughes AE (1999) Haploinsufficiency of desmoplakin causes a striate subtype of palmoplantar keratoderma. Hum Mol Genet 8:143–148

Asimaki A, Syrris P, Ward D, Guereta LG, Saffitz JE, McKenna WJ (2009) Unique epidermolytic bullous dermatosis with associated lethal cardiomyopathy related to novel desmoplakin mutations. J Cutan Pathol 36:553–559

Ast G (2004) How did alternative splicing evolve? Nat Rev Genet 5:773–782

Boguski MS, Lowe TM, Tolstoshev CM (1993) dbEST–database for "expressed sequence tags". Nat Genet 4:332–333

Bolling MC, Jonkman MF (2009) Skin and heart: une liaison dangereuse. Exp Dermatol 18:658–668

Bornslaeger EA, Corcoran CM, Stappenbeck TS, Green KJ (1996) Breaking the connection: displacement of the desmosomal plaque protein desmoplakin from cell-cell interfaces disrupts anchorage of intermediate filament bundles and alters intercellular junction assembly. J Cell Biol 134:985–1001

Bornslaeger EA, Godsel LM, Corcoran CM, Park JK, Hatzfeld M, Kowalczyk AP, Green KJ (2001) Plakophilin 1 interferes with plakoglobin binding to desmoplakin, yet together with plakoglobin promotes clustering of desmosomal plaque complexes at cell-cell borders. J Cell Sci 114:727–738

Bustin SA (2000) Absolute quantification of mRNA using real-time reverse transcription polymerase chain reaction assays. J Mol Endocrinol 25:169–193

Cabral R, South A (2009) Inherited disease of the desmosome. In: Cirillo N (ed) Pathophysiology of the desmosome. Research Signpost, Kerala, pp 121–156

Fontao L, Favre B, Riou S, Geerts D, Jaunin F, Saurat JH, Green KJ, Sonnenberg A, Borradori L (2003) Interaction of the bullous pemphigoid antigen 1 (BP230) and desmoplakin with intermediate filaments is mediated by distinct sequences within their COOH terminus. Mol Biol Cell 14:1978–1992

Franke WW, Moll R, Schiller DL, Schmid E, Kartenbeck J, Mueller H (1982) Desmoplakins of epithelial and myocardial desmosomes are immunologically and biochemically related. Differentiation 23:115–127

Franke WW, Borrmann CM, Grund C, Pieperhoff S (2006) The area composita of adhering junctions connecting heart muscle cells of vertebrates. I. Molecular definition in intercalated disks of cardiomyocytes by immunoelectron microscopy of desmosomal proteins. Eur J Cell Biol 85:69–82

Gallicano GI, Kouklis P, Bauer C, Yin M, Vasioukhin V, Degenstein L, Fuchs E (1998) Desmoplakin is required early in development for assembly of desmosomes and cytoskeletal linkage. J Cell Biol 143:2009–2022

Getsios S, Huen AC, Green KJ (2004) Working out the strength and flexibility of desmosomes. Nat Rev Mol Cell Biol 5:271–281

Green KJ, Parry DA, Steinert PM, Virata ML, Wagner RM, Angst BD, Nilles LA (1990) Structure of the human desmoplakins. Implications for function in the desmosomal plaque. J Biol Chem 265:2603–2612

Green KJ, Stappenbeck TS, Noguchi S, Oyasu R, Nilles LA (1991) Desmoplakin expression and distribution in cultured rat bladder epithelial cells of varying tumorigenic potential. Exp Cell Res 193:134–143

Green KJ, Stappenbeck TS, Parry DA, Virata ML (1992) Structure of desmoplakin and its association with intermediate filaments. J Dermatol 19:765–769

Hebsgaard SM, Korning PG, Tolstrup N, Engelbrecht J, Rouze P, Brunak S (1996) Splice site prediction in *Arabidopsis thaliana* pre-mRNA by combining local and global sequence information. Nucleic Acids Res 24:3439–3452

Johnson JM, Castle J, Garrett-Engele P, Kan Z, Loerch PM, Armour CD, Santos R, Schadt EE, Stoughton R, Shoemaker DD (2003) Genome-wide survey of human alternative pre-mRNA splicing with exon junction microarrays. Science 302:2141–2144

Jonkman MF, Pasmooij AM, Pasmans SG, Berg MP van den, Ter Horst HJ, Timmer A, Pas HH (2005) Loss of desmoplakin tail causes lethal acantholytic epidermolysis bullosa. Am J Hum Genet 77:653–660

Kinsella TM, Nolan GP (1996) Episomal vectors rapidly and stably produce high-titer recombinant retrovirus. Hum Gene Ther 7:1405–1413

Kouklis PD, Hutton E, Fuchs E (1994) Making a connection: direct binding between keratin intermediate filaments and desmosomal proteins. J Cell Biol 127:1049–1060

Kowalczyk AP, Stappenbeck TS, Parry DA, Palka HL, Virata ML, Bornslaeger EA, Nilles LA, Green KJ (1994) Structure and function of desmosomal transmembrane core and plaque molecules. Biophys Chem 50:97–112

Kowalczyk AP, Bornslaeger EA, Borgwardt JE, Palka HL, Dhaliwal AS, Corcoran CM, Denning MF, Green KJ (1997) The amino-terminal domain of desmoplakin binds to plakoglobin and clusters desmosomal cadherin-plakoglobin complexes. J Cell Biol 139:773–784

Kowalczyk AP, Hatzfeld M, Bornslaeger EA, Kopp DS, Borgwardt JE, Corcoran CM, Settler A, Green KJ (1999) The head domain of plakophilin-1 binds to desmoplakin and enhances its recruitment to desmosomes. Implications for cutaneous disease. J Biol Chem 274:18145–18148

Matlin AJ, Clark F, Smith CW (2005) Understanding alternative splicing: towards a cellular code. Nat Rev Mol Cell Biol 6:386–398

Meng JJ, Bornslaeger EA, Green KJ, Steinert PM, Ip W (1997) Two-hybrid analysis reveals fundamental differences in direct interactions between desmoplakin and cell type-specific intermediate filaments. J Biol Chem 272:21495–21503

Moll R, Sievers E, Hammerling B, Schmidt A, Barth M, Kuhn C, Grund C, Hofmann I, Franke WW (2009) Endothelial and virgultar cell formations in the mammalian lymph node sinus: endothelial differentiation morphotypes characterized by a special kind of junction (complexus adhaerens). Cell Tissue Res 335:109–141

Morgenstern JP, Land H (1990) Advanced mammalian gene transfer: high titre retroviral vectors with multiple drug selection markers and a complementary helper-free packaging cell line. Nucleic Acids Res 18:3587–3596

Mueller H, Franke WW (1983) Biochemical and immunological characterization of desmoplakins I and II, the major polypeptides of the desmosomal plaque. J Mol Biol 163:647–671

Norgett EE, Hatsell SJ, Carvajal-Huerta L, Cabezas JC, Common J, Purkis PE, Whittock N, Leigh IM, Stevens HP, Kelsell DP (2000) Recessive mutation in desmoplakin disrupts desmoplakin-intermediate filament interactions and causes dilated cardiomyopathy, woolly hair and keratoderma. Hum Mol Genet 9:2761–2766

Norgett EE, Lucke TW, Bowers B, Munro CS, Leigh IM, Kelsell DP (2006) Early death from cardiomyopathy in a family with autosomal dominant striate palmoplantar keratoderma and woolly hair associated with a novel insertion mutation in desmoplakin. J Invest Dermatol 126:1651–1654

North AJ, Bardsley WG, Hyam J, Bornslaeger EA, Cordingley HC, Trinnaman B, Hatzfeld M, Green KJ, Magee AI, Garrod DR (1999) Molecular map of the desmosomal plaque. J Cell Sci 112:4325–4336

O'Keefe EJ, Erickson HP, Bennett V (1989) Desmoplakin I and desmoplakin II. Purification and characterization. J Biol Chem 264:8310–8318

Parrish EP, Steart PV, Garrod DR, Weller RO (1987) Antidesmosomal monoclonal antibody in the diagnosis of intracranial tumours. J Pathol 153:265–273

Reese MG, Eeckman FH, Kulp D, Haussler D (1997) Improved splice site detection in Genie. J Comput Biol 4:311–323

Smith EA, Fuchs E (1998) Defining the interactions between intermediate filaments and desmosomes. J Cell Biol 141:1229–1241

South AP, Wan H, Stone MG, Dopping-Hepenstal PJ, Purkis PE, Marshall JF, Leigh IM, Eady RA, Hart IR, McGrath JA (2003) Lack of plakophilin 1 increases keratinocyte migration and reduces desmosome stability. J Cell Sci 116:3303–3314

Stappenbeck TS, Green KJ (1992) The desmoplakin carboxyl terminus coaligns with and specifically disrupts intermediate filament networks when expressed in cultured cells. J Cell Biol 116:1197–1209

Stappenbeck TS, Bornslaeger EA, Corcoran CM, Luu HH, Virata ML, Green KJ (1993) Functional analysis of desmoplakin domains: specification of the interaction with keratin versus vimentin intermediate filament networks. J Cell Biol 123:691–705

Stappenbeck TS, Lamb JA, Corcoran CM, Green KJ (1994) Phosphorylation of the desmoplakin COOH terminus negatively regulates its interaction with keratin intermediate filament networks. J Biol Chem 269:29351–29354

Uzumcu A, Norgett EE, Dindar A, Uyguner O, Nisli K, Kayserili H, Sahin SE, Dupont E, Severs NJ, Leigh IM, Yuksel-Apak M, Kelsell DP, Wollnik B (2006) Loss of desmoplakin isoform I causes early onset cardiomyopathy and heart failure in a Naxos-like syndrome. J Med Genet 43:e5

Valiron O, Chevrier V, Usson Y, Breviario F, Job D, Dejana E (1996) Desmoplakin expression and organization at human umbilical vein endothelial cell-to-cell junctions. J Cell Sci 109:2141–2149

Vasioukhin V, Bowers E, Bauer C, Degenstein L, Fuchs E (2001) Desmoplakin is essential in epidermal sheet formation. Nat Cell Biol 3:1076–1085

Virata ML, Wagner RM, Parry DA, Green KJ (1992) Molecular structure of the human desmoplakin I and II amino terminus. Proc Natl Acad Sci USA 89:544–548

Wan H, South AP, Hart IR (2007) Increased keratinocyte proliferation initiated through downregulation of desmoplakin by RNA interference. Exp Cell Res 313:2336–2344

Whittock NV, Ashton GH, Dopping-Hepenstal PJ, Gratian MJ, Keane FM, Eady RA, McGrath JA (1999) Striate palmoplantar keratoderma resulting from desmoplakin haploinsufficiency. J Invest Dermatol 113:940–946

Zhang Z, Schwartz S, Wagner L, Miller W (2000) A greedy algorithm for aligning DNA sequences. J Comput Biol 7:203–214